Prediction of the material with highest known melting point from *ab initio* molecular dynamics calculations

Qi-Jun Hong[*]

School of Engineering, Brown University, Providence, Rhode Island 02912, USA
and Division of Chemistry and Chemical Engineering, California Institute of Technology, Pasadena, California 91125, USA

Axel van de Walle

School of Engineering, Brown University, Providence, Rhode Island 02912, USA

Using electronic structure calculations, we conduct an extensive investigation into the Hf-Ta-C system, which includes the compounds that have the highest melting points known to date. We identify three major chemical factors that contribute to the high melting temperatures. Based on these factors, we propose a class of materials that may possess even higher melting temperatures and explore it via efficient *ab initio* molecular dynamics calculations in order to identify the composition maximizing the melting point. This study demonstrates the feasibility of automated and high-throughput materials screening and discovery via *ab initio* calculations for the optimization of "higher-level" properties, such as melting points, whose determination requires extensive sampling of atomic configuration space.

PACS number(s): 64.70.D−, 31.15.at, 31.15.E−, 81.05.Je

High-performance refractory materials [1–5] play an important role in applications ranging from gas turbines to heat shields for hypersonic vehicles. With melting points above 4000 K, hafnium carbide [6–12] and tantalum carbide [6,13,14] are among the most refractory binary compounds known to date [15]. Their mixture Ta_4HfC_5 melts at 4215 K [16], which has long been considered the highest melting temperature for any solid [17]. Very few measurements have been documented, because of the obvious experimental difficulties at extreme temperatures.

Computational approaches to melting point prediction offer exceptional control and monitoring of thermodynamic variables [18,19] and can more flexibly handle a wide range of materials and temperatures. However, a melting temperature calculation from quantum-mechanical methods has long been considered a challenging task, due to the requirement of extensive sampling of atomic configuration space, particularly for the liquid phase [20–22]. Given the computational burden of DFT [23], it is extremely difficult to perform systematic and high-throughput melting temperature calculations directly from first principles. We recently developed the small-size coexistence method [24,25], and managed to reduce the computer cost drastically. An automated computer code is prepared and freely distributed for direct DFT melting point calculations [25]. In this work, we apply the code to study these most refractory materials. We demonstrate that it is feasible to perform high-throughput materials screening and discovery directly via *ab initio* calculations for the optimization of melting point.

To help identify the factors leading to high melting points and validate our computational methodology, we first explore trends among known classes of refractories. Our investigation focuses on the rocksalt structure in the Hf-Ta-C systems, because it is the only stable solid-state form in the temperature region of melting [26,27]. Employing the small-cell coexistence method [24], we calculate the melting temperatures of

rocksalt HfC_x ($x \in [0.75,1]$), as shown in Fig. 1. Our calculations successfully capture the volcano-shape melting curve, which is widely observed in experiment [7,9–11], as well as the location of the apex (within 3 at. % of carbon content). Starting from stoichiometric HfC, the melting temperature increases along with carbon deficiency, until it reaches a maximum at the congruent melting point, near 45 at. % C ($HfC_{0.82}$). This feature explains why HfC undergoes carbon loss when it is heated and melted [29]: it remains in the solid state and loses carbon as the temperature increases. Further decrease in carbon composition leads to a drop of melting temperature.

It should be noted that our calculations identify the so-called midrib surface, that is, the temperature where the free energy of the solid and the liquid are equal at a given composition. The midrib surface generally lies between the solidus and liquidus, but agrees exactly with the melting point at extrema (where the solidus and liquidus meet), thus enabling us to accurately predict optimal melting points. As the calculations are performed under constant pressure conditions, they can determine whether the solid melts or sublimes and only melting is observed. However, the calculations do not include the possible effects of an oxygen-rich environment (carbon loss via oxidation) and are thus representative of heating under an inert atmosphere (e.g., nitrogen).

We note that the vertical shift of the calculated melting curve, relative to experiment, does not appear to be composition-dependent and thus does not significantly affect trends. This shift amounts to about 5% of the melting temperature itself, which is typical for DFT calculations. In addition to the Perdew-Burke-Ernzerhof (PBE) functional [30], which we employed for melting temperature calculations, we have cross-checked a subset of data points with a generally more accurate, but considerably more expensive, Heyd-Scuseria-Ernzerhof (HSE) hybrid functional [31] and found an average shift upward by +460 K (see Table I in Ref. [25]). The fact that PBE and HSE-based results bracket the experimental data further verifies that the error is mostly caused by the drawback of DFT exchange-correlation functionals, which is understandable given the nontrivial electronic structure of HfC

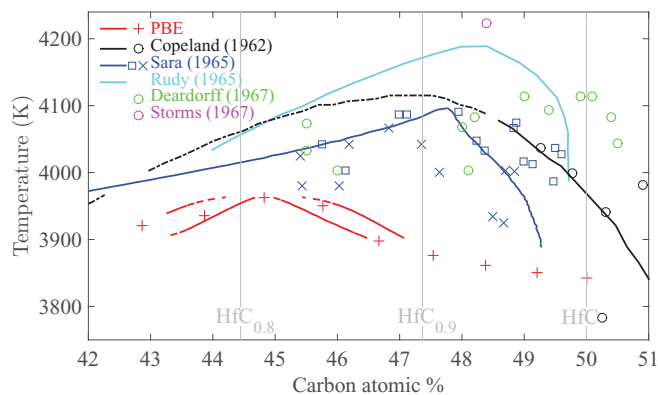*Corresponding author: qijun_hong@brown.edu

FIG. 1. (Color) The Hf-C phase diagram. Prior experimental measurements of the melting points are compared with the present computational results (labelled "PBE" as they rely on the PBE functional). The temperatures where free energies of the liquid and of the solid intersect are marked by "+". Also shown are the solidus and liquidus obtained via a CALPHAD model [28] fitted to our calculated thermodynamic data. Our calculations successfully capture the location of the apex within 3 at. % of carbon content. The vertical shift in calculated temperature, relative to experimental data, is essentially composition-independent and mostly reflects DFT error (see discussion in text).

and the extremely high temperature. Despite the considerable difference between PBE and HSE results, we note that all melting point calculations are based on the PBE functional in this article. Therefore the trend of melting temperature change is still valid and consistent, and the comparison of melting temperature remains effective, as all calculations are carried out with the same DFT functional.

The high melting temperature of hafnium carbide is primarily (through the well-known relation $T_m = \Delta H / \Delta S$) due to its exceptionally large fusion enthalpy of 0.81 eV atom^{-1}, a value usually unparalleled among refractories. (For reference, Al_2O_3 (m.p. 2345 K): 0.22; W (m.p. 3695 K): 0.37; Hf (m.p. 2506 K): 0.26 eV atom^{-1}). Indeed, a large heat of fusion is the first and most prominent factor we find that contributes to a high melting point. The chemical origin of the remarkably large heat of fusion can be studied via a wave-function analysis. While most researchers agree that the Hf-C interatomic bonding is a mixture of metallic, covalent and ionic interactions, its precise nature has not been well understood [32–34]. The system's wave functions, illustrated in Fig. 2, reveal numerous types of chemical interactions, including Hf–Hf 5d σ bond, C–C 2p σ bond and Hf 5d-C 2p π bond. This diversity enables each atom to bind with all its first- *and* second-nearest neighbors, thus forming an unusually large number of bonds and promoting the formation of a deep valence band (see Fig. 2). These bonds also carry both covalent and ionic characters. On one hand, the decomposed density of states (Fig. 2) shows contribution from both carbon and hafnium, hence demonstrating a typical covalent bond pattern. On the other hand, charge density analysis (Fig. 3) clearly shows partial charge transfer from hafnium to carbon, a strong evidence of ionic bonding, which is confirmed by a Bader charge analysis [35] indicating a 0.62 e charge transfer.

The second contributor we recognize is the presence of point defects, which affect melting temperature via entropy.
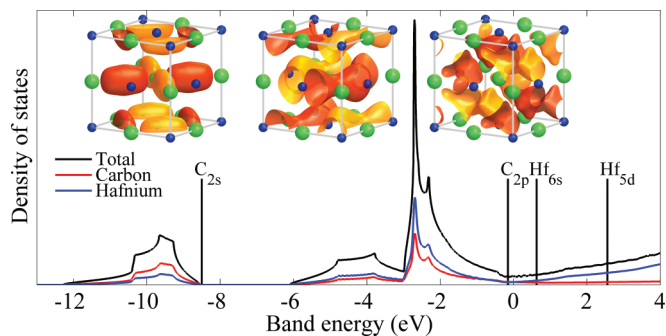

FIG. 2. (Color) Electronic density of states in HfC showing clear participation of both Hf and C in forming covalent bonds. Total density of states is shown in black. Projections on C and Hf are colored in red and blue, respectively. The Fermi level is at 0. Vertical lines are energy levels of atomic orbitals. Insets are wave functions illustrating the diversity of bond types in HfC with clear covalent character. From left to right, these figures represent Hf 5d σ bond, C 2p σ bond, and Hf 5d–C 2p π bond. Surfaces of constant value of the real parts of the wave functions are represented. Hf and C atoms are colored in green and blue respectively.

More generally, we find that, at high temperatures, entropic effects favor and stabilize a considerable amount of lattice defects. When solid HfC becomes off-stoichiometric HfC$_{1-x}$, the presence of carbon vacancies increases the configurational entropy (e.g., for an ideal lattice solution, $S = -k \sum_i x_i \ln x_i$), and this benefit is further magnified by the high temperature ($G = H - TS$). If this entropic effect more than offsets the defect formation energy penalty, these vacancies stabilize the solid phase. Since, by definition, vacancies can only exist in the solid phase, this effect is absent in the liquid and the net effect would be an increase in melting temperature. While this argument appears contradictory to the Lindemann melting criterion [36], we note that it is actually complementary. By empirically correlating melting with the amplitude of thermal vibration, the Lindemann's rule focuses on the solid structure, and it lacks a thermodynamic awareness of both the solid and
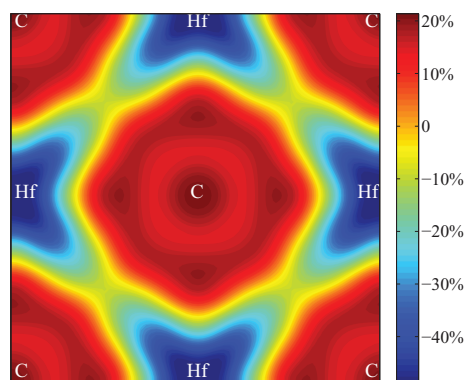

FIG. 3. (Color) The electron transfer in HfC. The figure reports $\rho/\rho_0 - 1$, where ρ is electronic charge density from DFT wave function and ρ_0 is initial overlapping atomic charge density. The sharp contrast clearly shows a charge transfer from Hf to C indicative of ionic interactions, although covalent character is still visible in the anisotropy of the charge density.

the liquid. Moreover, an overall evaluation needs to account for both energetic and entropic factors, in addition to the geometric structure. Though vacancies may facilitate melting by allowing larger displacements according to the Lindemann criterion, our calculation suggests that vacancies also increase the heat of fusion of HfC at low vacancy concentrations (see Fig. 2 in Ref. [25]). Therefore both energetic and entropic effects are in favor of a more stable solid phase in the presence of vacancies through a mechanism that acts independently of Lindemann's suggestion.

Indeed, this fact explains why melting point climbs when HfC becomes off-stoichiometric and carbon-deficient, a phenomenon widely observed in experiments (Fig. 1). Furthermore, this entropic effect becomes so large at high temperatures that it not only stabilizes defects, but facilitates their formation as well. For instance, we observe the formation of C_2 (two carbon atoms near one anion lattice site) and vacancy in MD simulations, especially for compositions close to stoichiometric HfC. These unstable C_2 complexes tend to leave the solid, which results in carbon loss of stoichiometric HfC.

The third chemical factor we identify is well exemplified in the Hf-Ta-C system. While binary carbides, such as HfC and TaC, are constrained by the given electronic properties of these metals, mixing two carbides provides an avenue to tune chemical properties. Hf and Ta share a similar electronic structure but a slightly different number of valence electrons, which allows tuning of the location of the Fermi level so that it lies precisely between the bonding and anti-bonding bands without distorting the density of states.

To investigate this effect, we calculate melting points of $Hf_xTa_{1-x}C_{0.875}$ at various compositions ($x = 0, 0.125, 0.25, 0.375, 0.5, 0.75, 0.81, 1$). Our choice of carbon content is based on a consensus of experimental data that maximize the melting points of the binary carbides. Because of the rapid evaporation of carbon at high temperatures, it is difficult to assign the measured melting point to the correct composition in experiments [12,29]. The maximal melting temperature in the Hf-C system falls in the $HfC_{0.85-0.95}$ region [7,9,10,12,29], while Ta-C has a strong tendency to lose carbon and the melting point maximum is near $TaC_{0.8-0.9}$ [12,14,29]. The Hf-Ta-C system contains $HfTa_4C_5$, which has long been considered the most refractory substance known to date [17]. Our computational results, in general, agree with Agte's experimental measurements [16], as shown in Fig. 4. Our calculation indeed captures a cusp near $HfTa_4C_5$ in the composition-dependence of the melting point. Our calculation provides more details at the Hf-rich region, which was not explored in Agte's experiment. Existing experimental data are controversial on the issue of whether HfC or TaC has a higher melting point. Agte found HfC and TaC have nearly the same melting temperature [16]. While Rudy's study showed that the melting point of TaC is about 50 K higher than that of HfC [14], Emeleus, on the contrary, claimed that HfC melts at least 100 K above TaC [15]. Our calculations suggest that the melting temperature of $HfC_{0.875}$ is ∼70 K higher than that of $TaC_{0.875}$. Given the difficulty in measuring melting points at such high temperatures and the melting point's sensitivity to the exact carbon content, which is also hard to control at high temperatures, these discrepancies are not surprising.
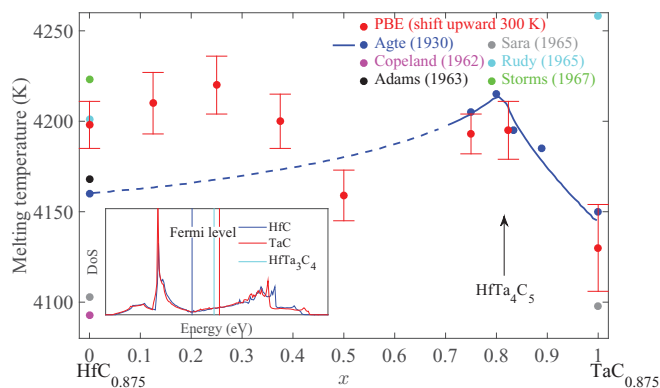

FIG. 4. (Color) Melting temperature of $Ta_xHf_{1-x}C_{0.875}$ as a function of x. Agte's measurements [16] focused on the Ta-rich side, while the rest part of the phase diagram was extrapolated as dash lines. Our melting point calculations provide more details at the Hf-rich region. The calculated melting curve captures the cusp near Ta_4HfC_5 (as the melting points of $Ta_{0.75}Hf_{0.25}C_{0.875}$ and $Ta_{0.81}Hf_{0.19}C_{0.875}$ are evidently higher than those of $Ta_{0.5}Hf_{0.5}C_{0.875}$ and $TaC_{0.875}$), which illustrates the effect of tuning the Fermi level via alloying, so that it lies precisely between the bonding and antibonding bands. The inset shows the effect on the Fermi level of the solid phase by tuning composition in $Ta_xHf_{1-x}C$. Vertical lines are Fermi levels. Our calculation suggests that the melting temperature of $HfTa_4C_5$, instead of being the highest, barely falls within the melting temperatures of the pure components, which corroborates Rudy's report [37].

Guided by the three contributing factors discussed above, we explore a new class of refractory materials, which may have higher melting temperatures than Hf-Ta-C. (1) We focus on isostructural alternatives to Hf-Ta-C, because the strong binding with both first and second-nearest neighbors is a very favorable feature we wish to maintain. For the same reason, we look for an alternate composition with similar cation/anion atomic radius ratios and similar electronegativity differences. (2) To preserve the ability to tune the Fermi level, we consider more than one element on both the cation and the anion sublattices and start with a composition space including Ta, Hf, B, C, and N. Adding more transition metals did not appear beneficial since the valence electron density of Ta and Hf already brackets the optimal Fermi level for the rocksalt crystal structure considered here. For the anions, atom size and electronegativity considerations (to preserve the rocksalt crystal structure) lead us to limit ourselves to $2p$ elements. (3) According to known melting temperatures of binary compounds (HfB: 2280 (decompose); HfN: 3660; TaB: 3360; TaN: 3370 K), we identified the Hf-C-N ternary subsystem as a promising candidate. HfN, a solid in rocksalt structure like HfC, has the highest melting temperature of all known metal nitrides. The high stability of both HfN and HfC suggests a thermally stable ternary system. Indeed, we find that the Hf-C-N system generally has a larger heat of fusion than HfC does. The Hf-C-N system was found thermodynamically stable [38], and the HfC-HfN mixture features complete solid solubility [39,40]. (4) To exploit possible entropic effects, we allow for vacancies on the anion sublattice.

Our calculations indicate that the Hf-C-N system includes materials that have higher melting points than any other
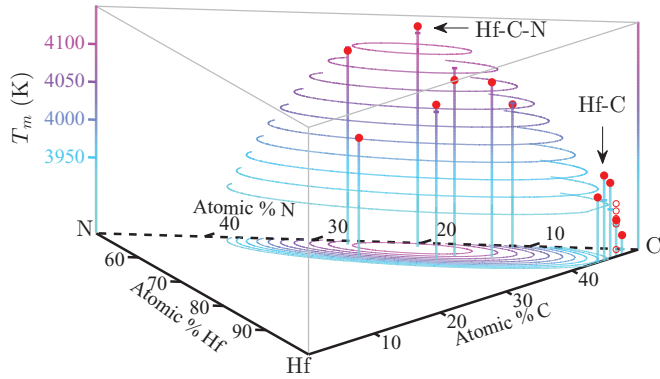
FIG. 5. (Color) Melting temperatures of Ta-Hf-C-N alloys. Filled circles mark the calculated melting temperatures in the Hf-C and Hf-C-N systems while open circles show data from the Ta-Hf-C system for comparison. The melting temperature surface $T_m(x_N, x_C)$ (shown as contour lines) was obtained via a regression analysis of the calculated melting temperatures based on a quadratic function of composition. See Table II in Ref. [25] for melting point data. A 2D version of the melting point surface is available in Fig. 1 in Ref. [25].

FIG. 6. (Color) Pair correlation function (normalized as $r \rightarrow \infty$) in liquid-state $Hf_{32}C_{24}N_7$. We find a remarkable difference between carbon and nitrogen: there is nearly no N–N (yellow) "near neighbors" (first pair correlation peak), compared to a considerable amount of C–C (red). The inset shows compositions of near neighbors for C and N atoms in liquid-state $Hf_{32}C_{24}N_7$ (the compositions of Hf–C and Hf–N account for the rest and are omitted). N atom has significantly less tendency to couple with C (2.17% vs 7.15%) and N (0.02% vs 0.59%).

substances known to date. As shown in Fig. 5, we find a large number of Hf-C-N mixtures, whose melting temperatures are significantly higher than the Hf-C and Hf-Ta-C systems. These new refractory materials increase the melting temperature record by up to 200 K. A regression analysis of our melting point data indicates that the highest melting point is located in the vicinity of $x_N = 0.20$ and $x_C = 0.27$ (where x subscript E denotes the atomic fraction of element E). We find that Ta does not help increase the melting temperature further.

In investigating this broader class of systems, we have observed another, independent, melting point-enhancing mechanism. We find that the addition of nitrogen remarkably changes the liquid structure and renders the phase less stable, which hinders melting. We explain this effect as follows. A liquid is more stable at a high temperature because it can access a much larger phase space, which contributes to a larger entropy that offsets its higher energy. In particular, the liquid allows for a richer variety of pairwise correlations. For instance, while there are only Hf–X ($X =$ C, N) nearest neighbors in solid-state Hf-C-N, additional pairs such as Hf–Hf and $X1$–$X2$ ($X1, X2 =$ C, N) are allowed in the liquid. This is an important entropic benefit in favor of the liquid phase, provided these new pairs do not entail too much energy penalty. We find that the main impact of the additional nitrogen is via the unstable C–N and N–N pairs, which is made clear in the following two analyses. First, we calculate the defect formation energy of X–X ($X =$ C,N) in the matrix of solid-state HfC as

$$\Delta E = E(\text{a } X\text{–}X \text{ pair on one anion lattice site})$$
$$+ E(\text{vacancy}) - 2E(X).$$

This quantity measures the energy cost to move a X atom from an anion sublattice site (leaving a vacancy at the site) to another anion (creating a X–X pair at the site). We find N–N has a much higher defect formation energy than C–C (5.8 versus 3.6 eV), which suggests a larger energy penalty when breaking Hf–N bonds to form N–N, a necessary step to melt the solid. As
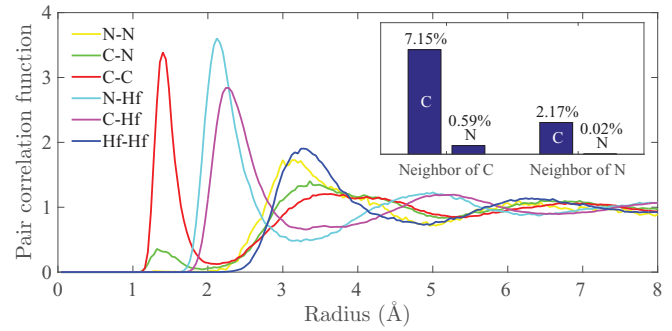
this process becomes less favorable with nitrogen added, the Hf-C-N system is harder to melt. Indeed, the heat of fusion is larger in the Hf-C-N system (Fig. 2 in Ref. [25]). Second, the pair-correlation function in Hf-C-N liquid (Fig. 6) shows dramatically lower occurrence of C–N and N–N, compared to a considerable amount of C–C pairs. This is also due to the higher formation energy of these two pairs. Indeed, a nitrogen atom has significantly less tendency than carbon (Fig. 6) to couple with the anions (C and N). The addition of nitrogen atoms largely reduces the number of anion-anion pairs in the liquid, forcing them to bind with Hf. This constraint limits the accessible phase space of the liquid and thus reduces its entropy. Figure 3 in Ref. [25] formally quantifies this effect in the Hf-C-N system. The relative instability of the N–N bond may appear strange at first, as the nitrogen molecule (N_2) is usually considered very stable. However, when a N–N complex is bound to other atoms, its stability can significantly decrease, as commonly observed in other compounds. For example, azide, a common compound with an anion N_3^-, is usually explosive; hydrazine (N_2H_4) is used as high-energy rocket fuels; dinitrogen tetroxide (N_2O_4) easily undergoes decomposition to its monomer (NO_2) under room temperature.

In summary, we have performed *ab initio* electronic structure calculations to study the Hf-C and Hf-Ta-C systems, which hold the highest melting temperatures known to date. The *ab initio* methods enable us to freely explore new compositions in a complex multicomponent system without the demanding prerequisite to develop new empirical potentials. The first-principles electronic structure theory also naturally captures the electronic effects driven by the position of Fermi level, while empirical potentials usually fail to do so. We have identified and investigated three factors responsible for the exceptionally high melting points in a class of transition metal carbides: (i) the presence of a large number of strong bonds between both nearest and second-nearest neighbors that exhibit a mixture of strong covalent and strong ionic characters; (ii) the entropy contribution of point defects that can exist in the solid but in the liquid (such as vacancies); and (iii) the

ability to tune, via alloying, the position of the Fermi level so that it lies just between the bonding and antibonding bands. These observations suggest the exploration of the Ta-Hf-C-N system in order to further increase the melting point. Our calculations suggest that a Hf-C-N alloy with 20 at. % of N and 27 at. % of C increases the current melting point record by up to 200 K and identify a melting point increase mechanism mediated by changes in pair correlation functions.

[1] N. P. Padture, M. Gell, and E. H. Jordan, Thermal barrier coatings for gas-turbine engine applications, Science **296**, 280 (2002).

[2] J. H. Perepezko, The hotter the engine, the better, Science **326**, 1068 (2009).

[3] K. Lu, The future of metals, Science **328**, 319 (2010).

[4] G. Liu, G. J. Zhang, F. Jiang, X. D. Ding, Y. J. Sun, J. Sun, and E. Ma, Nanostructured high-strength molybdenum alloys with unprecedented tensile ductility, Nat. Mater. **12**, 344 (2013).

[5] E. Wuchina, E. Opila, M. Opeka, W. Fahrenholtz, and I. Talmy, UHTCs: Ultra-high temperature ceramic materials for extreme environment applications, Electrochem. Soc. Interface **16**, 30 (2007).

[6] W. M. Haynes, *CRC Handbook of Chemistry and Physics*, 93rd ed. (CRC Press, Boca Raton, FL, USA, 2012), pp. 4-65 and 4-93.

[7] H. Kato and M. I. Copeland, Report of Investigations, U. S. Bureau of Mines, Report U-952 (1962).

[8] R. P. Adams and R. A. Beall, Preparation and evaluation of fused hafnium carbide. Report of Investigations, U. S. Bureau of Mines, Report 6304 (1963).

[9] R. V. Sara, The hafnium-carbon system, Trans. Metall. Soc. AIME **233**, 1683 (1965).

[10] E. Rudy and S. Windisch, Ternary phase equilibria in transition metal-boron-carbon-silicon systems, AFML-TR-65-2, Part 1, Vol IV (1965).

[11] D. K. Deardorff, M. I. Copeland, and R. P. Adams, The hafnium-carbon phase diagram. Report of Investigations, U. S. Bureau of Mines, Report 6983 (1967).

[12] E. K. Storms, *The Refractory Carbides* (Academic, New York, 1967), pp. 37–40, 83–87.

[13] R. V. Sara and C. E. Lowell, Wright Air Development Division of Materials and Processes, Progress Report WADD-TDR-60-143, Part V (1964).

[14] E. Rudy and D. P. Harmon, Ternary phase equilibria in transition metal-boron-carbon-silicon systems, AFML-TR-65-2, Part 1 Vol V (1965).

[15] H. J. Emeleus and A. G. Sharpe, *Advances in Inorganic Chemistry and Radiochemistry* (Academic, New York, 1968), Vol. 11, p. 167–175.

[16] V. C. Agte and H. Altertum, Untersuchungen über systeme hochschmelzender carbide nebst beiträgen zum problem der kohlenstoffschmelzung, Z. Tech. Physik. **11**, 182 (1930).

[17] Hafnium, *in Encyclopedia Britannica* (Encyclopedia Britannica, Chicago, 1993) retrieved from, http://www.britannica.com/science/hafnium.

[18] A. Samanta, M. E. Tucherman, T.-Q. Yu, and W. E, Microscopic mechanisms of equilibrium melting of a solid, Science **346**, 729 (2014).

[19] A. van de Walle, Simulations provide a rare look at real melting, Science **346**, 704 (2014).

[20] D. Frenkel and B. Smit, *Understanding Molecular Simulation*, (Academic, San Diego, 1996).

[21] D. A. Kofke and P. T. Cummings, Quantitative comparison and optimization of methods for evaluating the chemical potential by molecular simulation, Mol. Phys. **92**, 973 (1997).

[22] D. Alfè, M. J. Gillan, and G. D. Price, The melting curve of iron at the pressures of the Earth's core from *ab initio* calculations, Nature (London) **401**, 462 (1999).

[23] W. Kohn and L. J. Sham, Self-consistent equations including exchange and correlation effects, Phys. Rev. **140**, A1133 (1965).

[24] Q.-J. Hong and A. van de Walle, Solid-liquid coexistence in small systems: A statistical method to calculate melting temperatures, J. Chem. Phys. **139**, 094114 (2013).

[25] See Supplemental Material at http://link.aps.org/supplemental/10.1103/PhysRevB.92.020104 for details on the small-cell coexistence method, the SLUSCHI (Solid and Liquid in Ultra Small Coexistence with Hovering Interfaces) code, and the melting temperature calculations in this work. SLUSCHI is available at blogs.brown.edu/qhong.

[26] H. Okamoto, C-Hf (Carbon-Hafnium), *Binary Alloy Phase Diagrams*, edited by T. B. Massalski, 2nd ed. (ASM International, Materials Park, Ohio, 1990), Vol. 1, p. 849-852.

[27] A. I. Gusev, A. S. Kurlov, and V. N. Lipatnikov, Atomic and vacancy ordering in carbide ζ-Ta$_4$C$_{3-x}$($0.28 \leqslant x \leqslant 0.40$) and phase equilibria in the Ta-C system, J. Solid State Chem. **180**, 3234 (2007).

[28] L. Kaufman, Computational thermodynamics and materials design, CALPHAD: Comput. Coupling Phase Diagrams Thermochem. **25**, 141 (2001).

[29] R. A. Andrievskii, N. S. Strel'nikova, N. I. Poltoratskii, E. D. Kharkhardin, and V. S. Smirnov, Melting point in systems ZrC-HfC, TaC-ZrC, TaC-HfC, Soviet Powder Metall. Metal Ceram. **6**, 65 (1967).

[30] J. P. Perdew, K. Burke, and M. Ernzerhof, Generalized gradient approximation made simple, Phys. Rev. Lett. **77**, 3865 (1996).

[31] J. Heyd, G. E. Scuseria, and M. Ernzerhof, Hybrid functionals based on a screened Coulomb potential., J. Chem. Phys. **118**, 8207 (2003).

[32] R. Davis, *Advances in Ceramics, Vol. 23: Nonstoichiometric Compounds*, edited by Catlow CR, Mackrodt WC (The American Ceramic Society, Westerville, 1987), p. 529.

[33] V. A. Gubanov, A. L. Ivanovsky, and V. P. Zhukov, Electronic structure, chemical bonding and properties of binary carbides. *Electronic Structure of Refractory Carbides and Nitrides*, (Cambridge University Press, Cambridge, UK, 1994), p. 18–29.

[34] M. E. Eberhart, and J. M. MacLaren, The origins of the similarities between late transition metals and early transition metal monocarbides. *The Chemistry of Transition Metal Carbides and Nitrides*, edited by Oyama ST (Chapman and Hall, London, UK, 1996), pp. 107–120.

[35] G. Henkelman, A. Arnaldsson, and H. Jonsson, A fast and robust algorithm for Bader decomposition of charge density, Comp. Mater. Sci. **36**, 354 (2006).

[36] F. A. Lindemann, The calculation of molecular vibration frequencies, Physik. Z. **11**, 609 (1910).

[37] E. Rudy, Ternary phase equilibria in transition metal-boron-carbon-silicon systems, AFML-TR-65-2, Part 2, Vol I (1965).

[38] S. Binder, W. Lengauer, P. Ettmayer, J. Bauer, J. debuigne, and M. Bohn, Phase equilibria in the systems Ti-C-N, Zr-C-N and Hf-C-N, J. Alloy Compd. **217**, 128 (1995).

[39] C. Agte and K. Moers, Methoden zur reindarstellung hochschmelzender Carbide, Nitride und Boride und beschreibung einiger ihrer eigenschaften, Anorg. Allg. Chem. **198**, 233 (1931).

[40] R. Kieffer, H. Nowotny, P. Ettmayer, and G. Dufek, Neue untersuchungen über die mischbarkeit von übergangsmetallnitriden und -karbiden, Metall (Berlin) **26**, 701 (1972).